INT 187/94 July 1994

THE INTERFEROMETER OF TCV

C. Nieswand, S. Barry, R. Behn

Application for cost-sharing action
University College Cork
January 1994

Experts Group Meeting
August 22, 1994 at the CRPP-Lausanne

The Interferometer of TCV

C.Nieswand, S.Barry, R.Behn

CENTRE DE RECHERCHES EN PHYSIQUE DES PLASMAS
Association EURATOM - Confédération Suisse
Av. des Bains 21 - CH - 1007 LAUSANNE

Lausanne, July 1994

The Interferometer of TCV

1. Introduction

The tokamak TCV is designed to allow for creating a large variety of different plasmas. The parameter range is extremely large: the line averaged electron density will be some $10^{19}m^{-3}$ during ECRH heating experiment and has already reached $1.7 \cdot 10^{20}m^{-3}$ in other experiments. The maximum plasma current up to now was 800kA and can be increased up to 1MA in the future. The cross-section of the plasma can be circular, elliptical (elongation up to 3), D-shaped or the plasma may have one or two X-points at almost arbitrary postion in the vessel.
One of the main topics of the TCV experiment is the study of the stability of highly elongated plasmas. Transport phenomena will also be investigated in detail. In a later phase 4.5 MW ECRH will be installed to study heating and current drive.
The knowledge of the density profile of tokamak plasmas is essential.
An interferometer can reveal the line integrated density profile in tokamaks very precisely. The reconstruction of density profiles however is difficult for non circular highly asymmetric plasmas. It requires either line density measurements from a large number of chords with different angles with respect to the plasma or additional informations from flux probes and evaluation by an equilibrium code.
At TCV we have installed an interferometer with vertical chords. Therefore we have expanded the laser beam to a slab like cross-section. Several interferometer systems on tokamaks prooved the feasibility of such systems [1,2,3,4,5] : MHD phenomena were observed [6] and density pulse propagation studies were performed [7]. The system is designed in a way that it is possible to add in a later phase horizontal interferometer or reflectometer chords in order to get more information about the vertical density distribution.
At TCV a sophisticated Thomson scattering system determines electron density and temperature profiles. However the temporal resolution is limited to 10ms and the reliability of this system is not (yet) sufficient to use it as a permanently running diagnostic. The density measurement depends very critically on the absolute calibration of the system. Therefore the interferometer measurements are used to calibrate the Thomson scattering density measurement.
An interferometer system with high temporal and spatial resolution is therefore indispensable for a reliable density profile measurement on TCV.
Furthermore for the density control during tokamak operation a reliable signal representing the plasma density must be available under all possible plasma conditions. The FIR interferometer can easily reveal this information.
This paper presents the state of the art of the TCV interferometer.
The manifold reasons leading to the choice of the laser system and its detailed description are presented in the first part.
It is followed by the description of the laser system and the optical system of the interferometer.
The possible types of detectors for the system are discussed.

After describing briefly the control of the system, the signal treatment and the data acquisition system is presented
Finally first measurements are shown.

2. Wavelength selection

The choice of the wavelength of the laser was determined by several limiting conditions.

1) Density gradients in the plasma which have a component perpendicular to the laser beam lead to beam refraction. The refraction angle for a single pass scales approximately with λ^2 and linearly with the central electron density (assuming a parabolic density profile) [8].
The refraction for some TCV plasmas was calculated with a ray tracing code. Parabolic density profiles were assumed. The results for 214.6μm wavelength are shown in Fig. 1 for a high density plasma with elongation of about 2.5. For a wavelength larger than 300μm the refraction becomes unacceptable.
First measurements with 4 channels show even at 214.6μm a decrease of the signal on the detectors during H mode plasmas with high densities which is due to refraction.

2) The number of fringes in a Michelson or Mach-Zehnder interferometer scales linearly with the wavelength and the central density [8].
The expected phase shift profiles for typical TCV plasmas were calculated and are shown in fig 2.
A reasonable value for the resolution of the phase measurement is 1/20 fringe. Since the resolution concerning central density measurement should be about $5 \cdot 10^{11} cm^{-3}$ (elongated plasma) the desired wavelength should be larger than 200μm.
If the wavelength is larger than 300μm the number of fringes increases rapidly in high density plasma and the probability to loose fringes with a real time fringe counter increases as well.

3) The fraction of a fringe induced by vibrations scales with $1/\lambda$.
Assuming that the sensitivity of the interferometer should be typically 1/20 fringe and the typical change of the optical path induced by vibrations is about 10μm a minimum wavelength of at least 200μm is required.
The vibration effect can of course be eliminated by a two wavelength arrangement. For the TCV interferometer an additional diode laser interferometer is planned which is only sensitive to the vibrations.

4) Since the system should be designed in a way that it can easily be upgraded to a polarimeter the Faraday rotation of the beam should be measurable with a sufficently good sensitivity.
The rotation angle is roughly proportional to the plasma density, the plasma current and to the square of the wavelength. [8]
The precision which can be realized in such type of measurements is in the order of 0.1° rotation of the plane of polarization [9]. The maximum

rotation angle obtained with "standard" TCV plasmas should therefore be at least some degrees.
Results of some calculations for TCV are shown in figure 3. In these cases parabolic density and current density profiles were assumed.
For large rotation angles the birefringence of the plasma due to the toroidal magnetic field adds some ellipticity to the polarization of the probe beam which makes the interpretation of the results more difficult. Figure 4 shows the results obtained from calculations with the same plasma used in figures 1-3. For Faraday rotation angles larger than 30° at a wavelength of 214.6μm the ellipticity becomes approximately 0.02 which is still acceptable. Since the ellipticity scales with λ^3, B_{tor}^2 and linearly with the central electron density 214.6μm seems to be the upper limit for the wavelength with respect to the ellipticity.
It is obvious that especially for the Faraday rotation the optimum conditions for all possible plasma configuration cannot be fullfilled with a single wavelength. For example a plasma with $2 \cdot 10^{19} m^{-3}$ central density and 500kA current will produce a Faraday rotation of only 1.5° using a wavelength of 214.6μm while the upper limit of 30° is already reached at $2 \cdot 10^{20} m^{-3}$ and 1MA.
However for most standard TCV plasmas we found that a wavelength of 214.6μm would be the best solution considering polarimetry.

The operational regime for an interferometer/polarimeter defined by the different constraints discussed above is shown in a I-n_e plot (figure 5).
We decided to select a wavelength which allows for interferometric operation about the full density range of TCV plasmas and which allows for reliable polarimetric measurements in as many cases as possible.
We came to the conclusion that the laser line at 214.6μm of CH_2F_2 is the best choice for our interferometer/polarimeter.

3. The laser

We use a CO_2 laser pumped cw FIR laser as radiation source for our interferometer. Optically pumped FIR lasers offer a larger flexibility in the choice of the wavelength than discharge excited lasers (HCN eg.). Furthermore parts for the system were already available at CRPP.
The duration of a TCV plasma can be up to 2 seconds. This is in the order of the thermal constants in typical CO_2 laser pumped FIR lasers. Therefore an actively stabilized cw system will be used. A chopped laser with cycle periods of some seconds would never reach a stable state during a tokamak discharge.
The laser line at 214.6μm in CH_2F_2 was first observed by Danielewics et al. [11] and was assigned to rotational transition in the molecule by Lachambre et al. [12] The gas is pumped by the 9R34 line of a CO_2 laser. The strong laser line at 214.6μm is polarized perpendicular to the CO_2 laser polarization. Simultaneously the FIR laser can emit a line at 287μm which is polarized parallel to the CO_2 laser polarization and is usually weaker. [11,12] Cascade transition at 230.2μm and 248.8μm were observed as well. [12] We observed that if the CO_2 laser emits only

a small amout of radiation at the 9R32 line the very strong laser lines at 184.6μm and 235.9μm were excited. [13] Multi line operation leads to a very unstable output due to line competition and cascade transition effects at 214.6μm.
The same laser line was used for the interferometers at the Varennes tokamak [14] and at ATF [3].
The pump laser is a PL4 Edinburgh Instruments CO_2 laser which emits about 38W cw at the 9R34 line. The laser was already used at CRPP for other experiments during the recent years.
A scematic drawing of the laser system is shown in figure 6.
The resonator of the FIR laser is formed by a flat gold coated copper mirror on the one side, two silicon plates on the other side which form a Fabry-Perot output coupler with variable reflectivity and by a 1.8m long pyrex tube with 25mm inner diameter. The FP output coupler helps to select only the 214.6μm line from all the lines mentioned above. The inner silicon plate of the FP output coupler is coated for high reflection at the CO_2 laser wavelength. The CO_2 laser beam is coupled into the FIR laser through a 2.5mm diameter hole in the copper mirror.
The output mirror system is mounted on a motorized translation stage and the copper mirror an a piezoelectric translation stage. Both mirror supports are mounted inside the vacuum system. The CO_2 laser beam enters the laser through a ZnSe Brewster window and the output window for the FIR is a 6mm thick TPX sheet.
The laser beam is linearly and horizontally polarized.
The standard laser stabilizer 295 from Edinburgh Intruments is used to tune the CO_2 laser frequency to a position which yields maximum FIR output of the system. The signal from a pyroelectric detector measuring the FIR output power of the laser system serves as input signal for the stabilizer. This stabilization is running all the time which results in a minor modulation of the FIR output power which is however negligable for the interferometer operation.
The length of the FIR laser resonator is controlled by a specially designed circuit. Therefore the cavity length is modulated by the piezo driven copper mirror with a frequency of about 123 Hz. The modulated FIR signal is measured by a Lock-In amplifier. Its output signal is used to move the output coupler by a stepper motor into the proper direction. This stabilization is switched off before a tokamak discharge to exclude distortion which can result from power changes when the motor is active.
Figure 7 shows the FIR output power as a function of the pressure of the laser gas. The maximum is at about 0.3mbar with a slow decrease to higher pressures. Since the pressure broadening of the gain profile and the suppresion of competeting lines at high pressures allows for more stable operation at high pressures the laser is usually operated at 0.3-0.5mbar. Even an increase of the pressure due to leakage of the system up to 0.5-1 mbar causes only a minor degradation of the output power. Therefore the laser can operate under sealed off conditions over a week although high vacuum technology was avoided in order to reduce the costs of the system.
The maximum stable power obtained directly at the output window was 100mW at 214.6μm.
After a warm-up time of about one hour the system did run over an entire day with sufficient high and stable power.

The laser beam is nearly gaussian and has a beam waist radius of about 8mm close to the output window of the laser.

4. The optical system of the interferometer

The interferometer is of Mach-Zehnder type. The probe beam passes the vacuum vessel from the bottom to the top. Above the exit window it is combined with the reference beam which is frequency shifted by a rotating grating. The detectors is placed above the TCV tokamak (figures 8 and 9).

a) Optical housing

The laser system is placed outside the tokamak security area in a separate room. The optical system of the interferometer is mounted in boxes attached to a stable support structure close to the tokamak.
The laser beam is guided through glas tubes of 25mm inner diameter over a distance of about 9m from the laser to the tokamak. The transmission of the system is lower (50%) than expected from preliminary experiments since the quality of the used tubes is poorer than the quality of the test tube. A depolarisation of some percent was observed which makes this way of transmission unfavourable for a polarimeter setup. The polarisation of the beam at TCV is parallel to the toroidal field (O-mode). The beam is coupled to the waveguides some centimeters behind the output window of the laser.
Since atmospheric absorption is significant at 214.6μm ($0.4m^{-1}$on "normal" days) waveguides and boxes are flushed with dry air or dry nitrogen.
In order to minimize vibrations the support structure close to TCV (which serves also as the support structure for the Thomson scattering experiment at TCV) is based on two 7m high concrete pillars on opposite sides of TCV which are fixed on the basement floor. The pillars are connected above the machine by a bridge structure made of a fibreglass composite material. The boxes containing the interferometer optics are made from Fibrelam which is a fibreglass material with honeycomb structure. This provides high stability and low weight simultaneously. The boxes are attached to the pillars and the bridge structure forming a C frame enclosing the vacuum chamber of TCV. The whole structure does not touch the support structure, the coils or the vacuum chamber of TCV in order to avoid the transmission of any vibrations from the tokamak.
The structure including waveguides and boxes is shown in figures 8 and 9.

b) Beam path and optics

The laser beam enters the boxes which are attached to the large support structure at TCV and which contain the optical elements for the interferometer through the 25mm diameter waveguide. The beam is split into two almost equal parts immediately after leaving the waveguide.

The sperical mirrors δ and ε (see figure 9) determine the size of the probe beam in the vessel in toroidal direction. The cylindrical mirrors ζ and η expand the probe beam in radial direction up to the full size of the windows. Mirror η is in fact segmented and consists of three idendical cylindrical mirrors. The choice of cylindrical mirrors was determined by their fast availability and relative low costs. Meanwhile we are able to machine parabolic mirrors in our workshop and we made already sets of parabolic mirrors which will replace those cylindrical mirrors very soon.
The reference beam is frequency shifted by a rotating grating. The maximum achievable shift is 100kHz. The spherical mirrors λ and μ determine the size of the beam in toriodal direction whereas mirrors π and ρ (still cylindrical, soon parabolic) expand the reference beam up to the same size as the probe beam in radial direction.
Reference and probe beam are superposed on the beam combiner σ which is presently made of severall crystal quartz plates. Their thickness is chosen such that the transmission and reflection under 45° incidence is about equal.
The parameters of probe and reference beam 1m behind the beam combiner σ are listed in table 1. The parameters off the used mirrors are listed in table 2.
The chords of integration are now only determined by the size and position of the collection optics of the detectors. Presently only 5 channels are installed. The number was limited by the available electronic equipment. The radial positions are at R= 755, 825, 890, 970, and 1000mm (plasma edge at 660 and 1140 mm). The first channel is presently not working.
On the detectors probe beat signals are produced by the superposition of the probe and reference beams.
A small fraction of the reference and the probe beam is superposed on a reference detector before the probe beam enters the plasma producing a reference beat signal.
The relative phases between the probe signals and the reference signals contain the information about the line integrated electron density of the plasma along the chords.

c) Windows
The vertical interferometer has access to the plasma in sector 12 of TCV through large windows on the bottom and the top of the machine. The windows are segmented into three equal openings (figure 10). We do not have access to the plasma at the very inner and outer edges (see figure 11).
The windows are mounted in a water cooled flange approximately 10cm apart from the vacuum vessel. Cooling was foreseen since the whole vacuum vessel of TCV will be heated up to 300°C or more. The flange however is designed in a way that in case of a failure of the active cooling the passive radiative cooling of the flange is sufficient to prevent the windows from breaking. The sealings are Viton O-rings which does not reduce the quality of the vacuum in TCV.
A shutter system prevents the windows from being coated during glow and surface conditioning plasmas in TCV.

For a future horizontal extension of the interferometer three horizontal ports in sector 12 are available (figure 11).
We chose crystal quartz as window material which has a high transmission at 214.6μm and in the visible and which is compatible with the vacuum and with temperature changes.
The thickness of the windows is 7.422mm ± 3μm which gives optimum transmission (86%) for 214.6μm. Additionally the transmission at 118.6μm and 447μm (two other laser lines which could eventually be used) is maximum (60% and 90% respectively).

d) Mirrors
Most mirrors are surface Al mirrors on glass substrats. They have optical quality to allow for He-Ne laser alignement. The large cylindrical mirrors are composed by three cylindrical mirrors with equal radius of curvature. Since the result is not satisfying we machined large parabolic aluminium mirrors in our workshop in order to replace the segmented spherical mirrors. The mirror supports are all made from nonmagnetic materials as aluminium or fibreglass material. To avoid eddy currents in the aluminium parts large parts are avoided or segmented by isolating material.

e) Beamsplitters
Beamsplitters are all made of crystal quartz. This gives best stability and allows for simple alignement withg a He-Ne-laser. However for polarimetric application with rotating polarisation planes the birefringence of crystal quartz makes this material unfavourable. For this application meshes seem to be the better choice.

f) Rotating grating
The rotating grating was already used for the interferometer at TCA. The diameter of the wheel is 24cm and it was designed for first order operation at 447μm. Since the wavelength for the TCV interferometer is approximately half as large the wheel can be used in second order operation at 214.6μm. We found that the efficiency is still larger than 50%.
It is possible to run the wheel with 20 rounds per second which will produce a frequency shift of 108kHz. The vibration level are low. In the present interferometer version the rotating grating is mounted on the support structure close to at TCV and does not run faster than 2rps (10.8kHz).

5. Detectors

In principle we had the choice between three different types of detectors: pyroelectric detectors, Schottky diodes and hot electron bolometer like Ge or InSb detectors.

a) Pyroelectric detectors.
Their main advantage is their high reliability and simple handling. Once they are installed they need no further maintenance. They are low price devices as well and operate at room temperature.

Furthermore they are not polarisation sensitive.
Their NEP however is usually in the order of some $10^{-9}W/Hz^{-1/2}$ at 1kHz and the responsivity is in the order of 1kV/W. The NEP increases however dramatically and the responsivity decreases fast towards frequencies larger than 10kHz.
Estimations of the expected incident power lead to the conclusion that for 100kHz operation pyroelectric detectors are not suitable.

b) Schottky diodes
Since they are operating at frequencies of 100kHz and lower they are usually used in the Video mode. In this case the NEP is comparable to the NEP of pyroelectric detectors. However the NEP gets better at higher frequencies. The responsivity is in the order of 10V/W.
The diodes are relatively expensive and the total cost scale nearly linearly with the number of elements.
Schottky diodes are room temperature devices.
They are usually mounted in a corner cube which defines the antenna characteristics of the diode. The alignement of the diodes is therefore critical.
The devices are polarisation sensitive which may cause problems for the polarimeter option depending on which measurement sceme will be chosen.
Onother disadvantage is the fact that the Schottky contact may be lost due to unproper handling, due to excess power incident on the diode or due to some magnetically induced currents in the diode. A skilled person must be available to repair a damaged diode immediately.

c) Hot electron bolometer
InSb detectors e.g. have an extremly low NEP. It is in the order of some $10^{-12}W/Hz^{-1/2}$ (@214.6μm) which is at least 3 orders of magnitude smaller than for pyroelectric detectors or Schottky diodes. The responsivity in this spectral region is still some 100V/W and the frequency response goes up to 750kHz.
The devices must be cooled to liquid He temperature.
Therefore a large part of the price is caused by the cryostat, while the elements themselves are comparable to or even cheaper than Schottky diodes. It is possible to put up to 15-20 detectors in a single cryostat. The price of the total system will be approximately the same as for a Schottky diode system of comparable size.
Since the elements are fixed in the cryostat and the cryostat have limited size additional optics or waveguides are necessary to focus the beams on the detectors. The flexibility concerning positioning of the detectors is therefore limited.
Their alignement is easy since they are not polarization sensitive and the radiation is collected by a simple Winston cone antenna.
The only necessary maintenance is the control of the He cooling. For the liquid Nitrogen cooling cheap automatic refill systems are available. The helium hold time for large cryostats is presently 1 month. Furthermore the cryostat must be evacuated from time to time by a turbomolecular pump.
The JET interferometer/polarimeter is partially equipped with InSb detectors [15] as well as the horizontal chord of the TEXTOR interferometer/polarimeter [16].

d) Present equipment
Presently the interferometer at TCV is equipped with pyroelectric detectors from Mullard since they have been available from the former interferometer on TCA. The beam power (0.1-0.5mW per channel) is just sufficient to produce a usefull signal on 4 of the 5 detectors. But the noise level (mainly detector noise) is just at the acceptable limit. The detectors limit the bandwidth of the system to 5-10kHz.

e) Future precautions
TCV will be heated by and ignited by powerfull gyrotron radiation between 39GHz and 140GHz. Therefore future detectors must be protected against excess power exiting the windows. This can be done by meshes with properly chosen dimensions or other filters.

6. System control

The laser stabilisation runs autonomously. The stabilisation parameters can be set by software from the TCV control system computers. The amplitude of the beat signal on a central chord is monitored permanently and the air dryer is activated automatically when the signal drops below an alarm level. Figure 12 shows the beat signal over an entire day of tokamak operation.

7. Signal treatment and data acquisition

The reference beat signal and the reference beat signal shifted by $\pi/2$ is mixed with the probe beat signals of each channel. The mixers produce signals which are proportional to the sine and to the cosine of the phase shift, respectively. This signals are acquired with sufficient time resolution by TRCF CAMAC modules which are read by the TCV data acquisition system MDS+. The phase and the line integrated density are reconstructed afterwards by software. The equilibrium code of TCV provides the plasma contour (last closed flux surface) and the poloidal flux which makes it possible to calculate the line averaged density along the vertical chords. Presently the 4 working channels allow only to fit the measurements to a function like $n_e(\psi)=n_{e0}(1-(1-\psi/\psi_0)^{\alpha})$. The values of α vary e.g. between 3 and 4 in X-point plasmas. The line integrated densities however can be implemented directly into the equilibrium code which is not yet done.
For a single central channel however a fringe counter provides a real time signal for the density feedback control of TCV during normal operation. This signal is acquired as well.

8. Performance and measurements

The temporal. resolution of the system was measured to be approximately 200-300μs determined at a sawtooth crash.
The spatial resolution is about 25mm in radial direction determined by the size of the collecting mirrors in front of the detectors.
The (detector) noise in the central channel is equivalent to $3\text{-}5 \cdot 10^{17} m^{-2}$ line integrated density which corresponds to the required accuracy as defined in chapter 2.
Vibrations are visible. The amplitude can reach moere than a tenth of a fringe (more than 20μm). The main source of these vibrations is identified: The optics of the Thomson scattering has metallic part very close (some centimeters) to the stabilization coils of TCV. Eddy currents are induced and produve magnetic fields which interact with the stray OH field. Since the Thomson scattering and the interferometer use a common support structure, the induced vibrations are transmitted to the interferometer and excite some fundamental frequencies of the interferometer system. The dominant frequencies lie around 40-100Hz. Therefore a compensating diode laser interferometer will be installed.
The maximum line averaged density observed up to now is $1.7 \cdot 10^{17} m^{-3}$.
Modes, sawteeth and ELMs can easily be detected with this interferometer system.
The interferometer is a standard diagnostic on TCV and is running permanently during days of tokamak operation.

Some measurements are presented in figures 13-16.
Figure 13 shows a locked mode during a limiter H-mode plasma. The outer channels (the two lower traces) are modulated with a phase of 180° relative to the inner trace while the central trace shows only a very small modulation.
Figure 14 shows the density behaviour during a long H-mode plasma. The lowest trace is a "peaking parameter", which is defined to be 1 for totally flat profile and lower than 1 for peaked profiles.
Figures 15 and 16 show fast profile changes due to sawteeth and ELMs in another H-mode plasma.

References

[1] E.J.Doyle, J.Howard, W.A.Peebles, and N.C.Luhmann,Jr.; Rev.Sci.Instrum. 57, 1945 (1986)

[2] G.A.Hallock, M.L.Gartman, R.L.Castles, K.Chiang, and A.S.Rahman; Rev.Sci.Instrum. 61, 2893 (1990)

[3] C.H.Ma, D.P.Hutchinson, and K.L.Vander Sluis; Rev.Sci.Instrum. 61, 2891 (1990)

[4] B.W.Rice; Rev.Sci.Instrum. 63, 5002 (1992)

[5] A.C.A.P.van Lammeren, S.K.Kim, and A.J.H.Donné; Rev.Sci.Instrum. 61, 2882 (1990)

[6] A.C.A.P.van Lammeren, J.C.M.Timmermans, G.M.D.Hogeweij, S.K.Kim, A.J.H.Donné, and RTP-team; Proceedings of the 18th European Conference on Nuclear Fusion and Plasma Physics, Berlin, Vol 15C, II-73 (1991)

[7] Sung K.Kim, D.L.Brower, W.A.Peebles, and N.C.Luhmann,Jr.; Rev.Sci.Instrum. 59, 1550 (1988)

[8] D.Véron in Inrafred and Millimeter Waves edited by K.J.Button; Academic Press, New York, 1979

[9] H.Soltwisch; Rev.Sci.Instrum. 57, 1939 (1986)

[10] H.Soltwisch; Messung der internen Magnetfeld-Struktur von Tokamak Plasmen; Internal report, KFA Jülich, Jül-2339 (1990)

[11] E.J.Danielewics, T.A.Galantowics, F.B.Foote, R.D.Reel, and D.T.Hodges; Optics Letters 4, 280 (1979)

[12] J-L. Lachambre, P.Bernard, and M.Gagne; IEEE Jour. Quant. Electr. QE-21, 282 (1985)

[13] E.J.Danielewics; Proc. 4th Int.Conf. IR&MMWaves, Miami, 203 (1979)

[14] Lachambre : Varennes tokamak interferometer (??)

[15] G.Braithwaite, N.Gottardi, G.Magyar, J.O'Rourke, J.Ryan, and D.Véron; Rev.Sci.Instrum. 60, 2825 (1989)

[16] H.Soltwisch, presented on the Frühjahrstagung of the Deutschen Physikalischen Gesellschaft, Greifswald (1993)

	Probe beam		Reference beam	
	toroidal	radial	toroidal	radial
w (beam radius)	17.1 mm	197 mm	17.2 mm	201 mm
R (radius of curvature)	$2 \cdot 10^3$ m	$-7 \cdot 10^3$ m	$1.8 \cdot 10^3$ m	$-5 \cdot 10^3$ m
z (dist. to beam waist)	-9 mm	46 m	-10 mm	69 m
w_0 (beam waist)	17.1 mm	196 mm	17.2 mm	200 mm

Table1 : Laser beam parameters 1m behind the beam combiner

Nr.	diam./mm	Rc/mm	angle /deg.	dist. to last object / mm
		probe beam		
α	50	Separator crystal quartz)	45	100 (to waveguide)
β	75	inf	45	150
γ	75	inf	51.65	905
δ	75	tang. -7000	6.65	514
ε	125	tang. 4000	17.75	1400
ζ	100x100	tang. 300 sag. inf	12.6	860
η	3x (140x100)	tang. 2500 sag. inf	39.85	1118
σ		Separator (crystal quartz)	45	4100
		ref beam		
α	50	Separator	45	100 (to waveguide)
θ	75	tang. 600	14.35	328
ι	rotating grating	sag. inf tang. -120	50	300
κ	75	tang. 600	14.55	300
λ	75	tang. -4500	15.85	416
μ	125	tang. 7000	30.65	2808
ξ	125	inf	31.9	806
π	100x100	tang. 350 sag. inf	7.05	2405
ρ	3x (140x100)	tang. 3800 sag. inf	50.25	1373
σ		Separator (crystal quartz)	45	650

Table 2 : Parameters of the most important optical elements of the TCV interferometer (see figure 9)

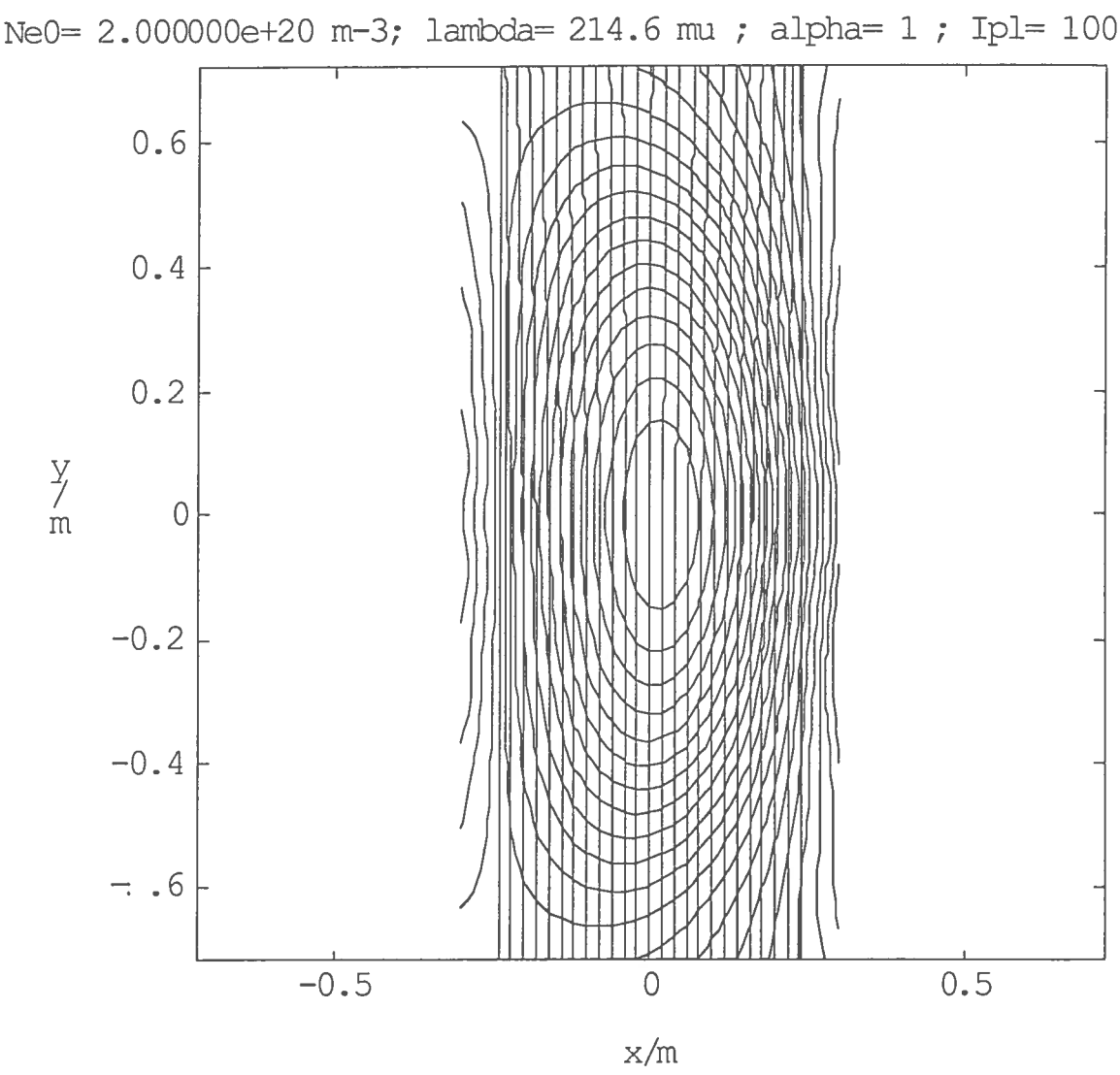

Fig. 1 : Refraction of a fan of rays at 214.6μm by a high density elliptical TCV plasma, parabolic density profile

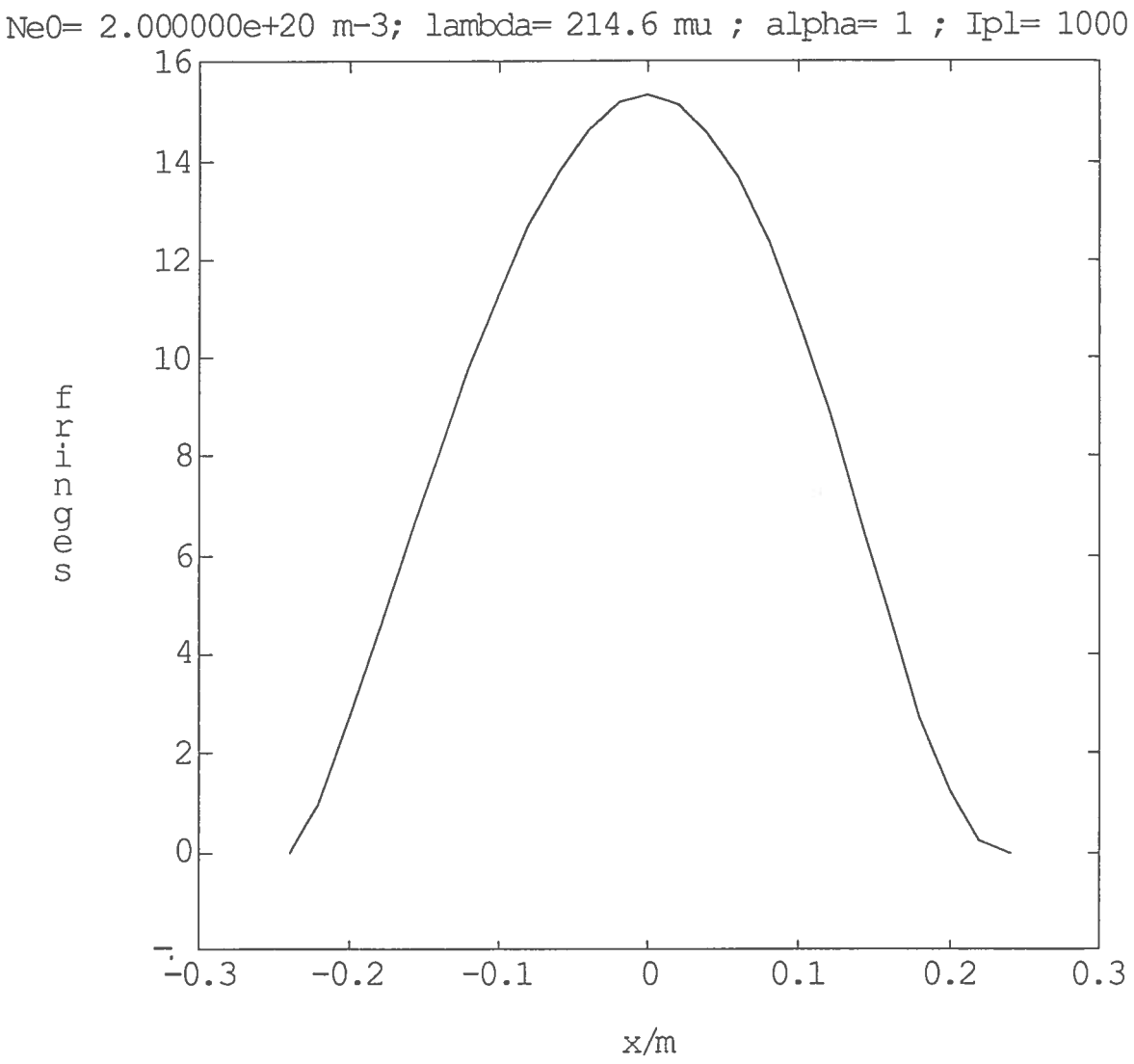

Fig. 2 : Phase shift profile in fringes for a high density elliptical TCV plasma (see fig.1). l = 214.6μm, parabolic density profile.

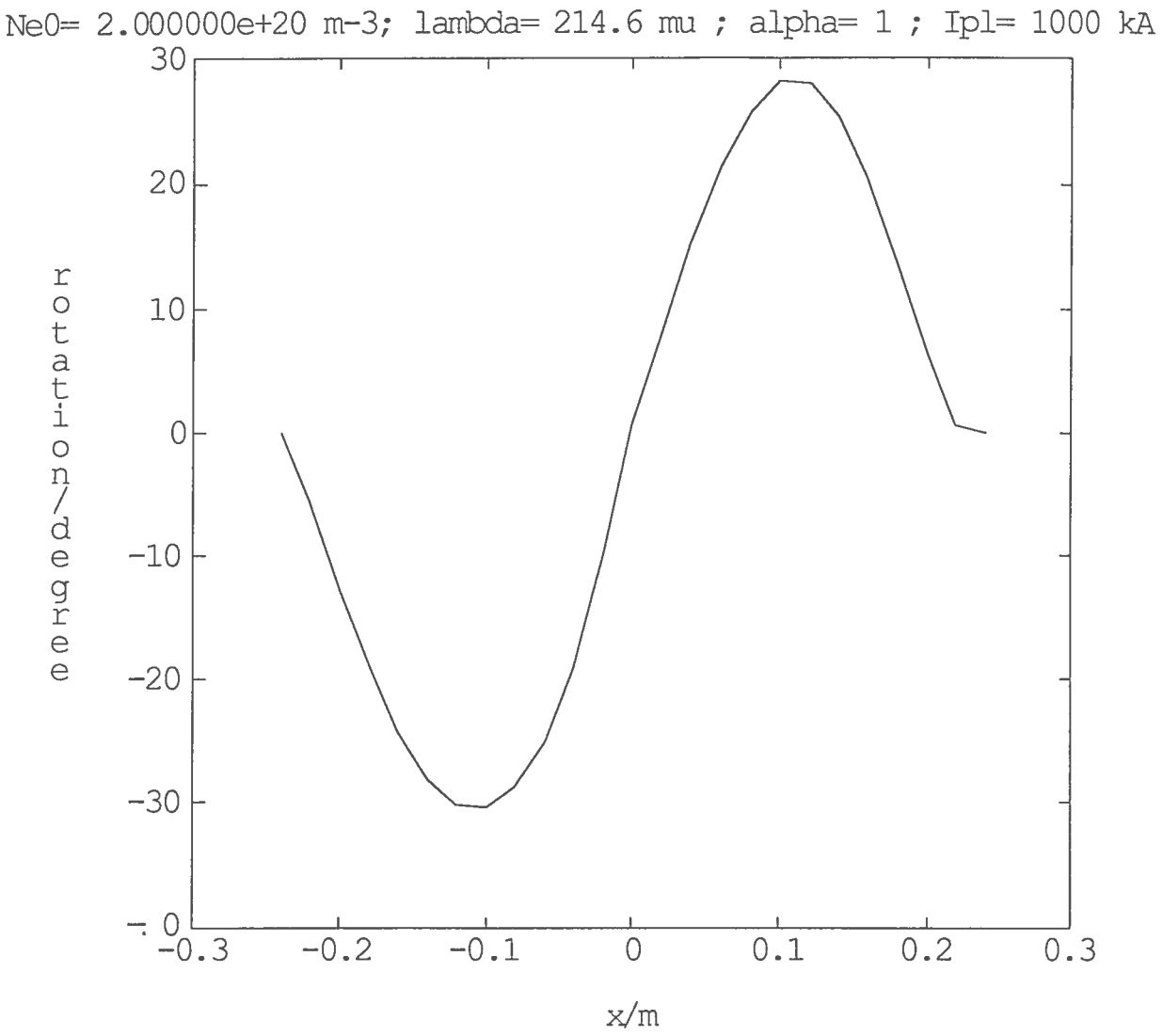

Fig. 3 : Faraday rotation angle for a high density elliptical 1MA TCV plasma (see fig.1), l=214.6μm, parabolic density and current density profiles.

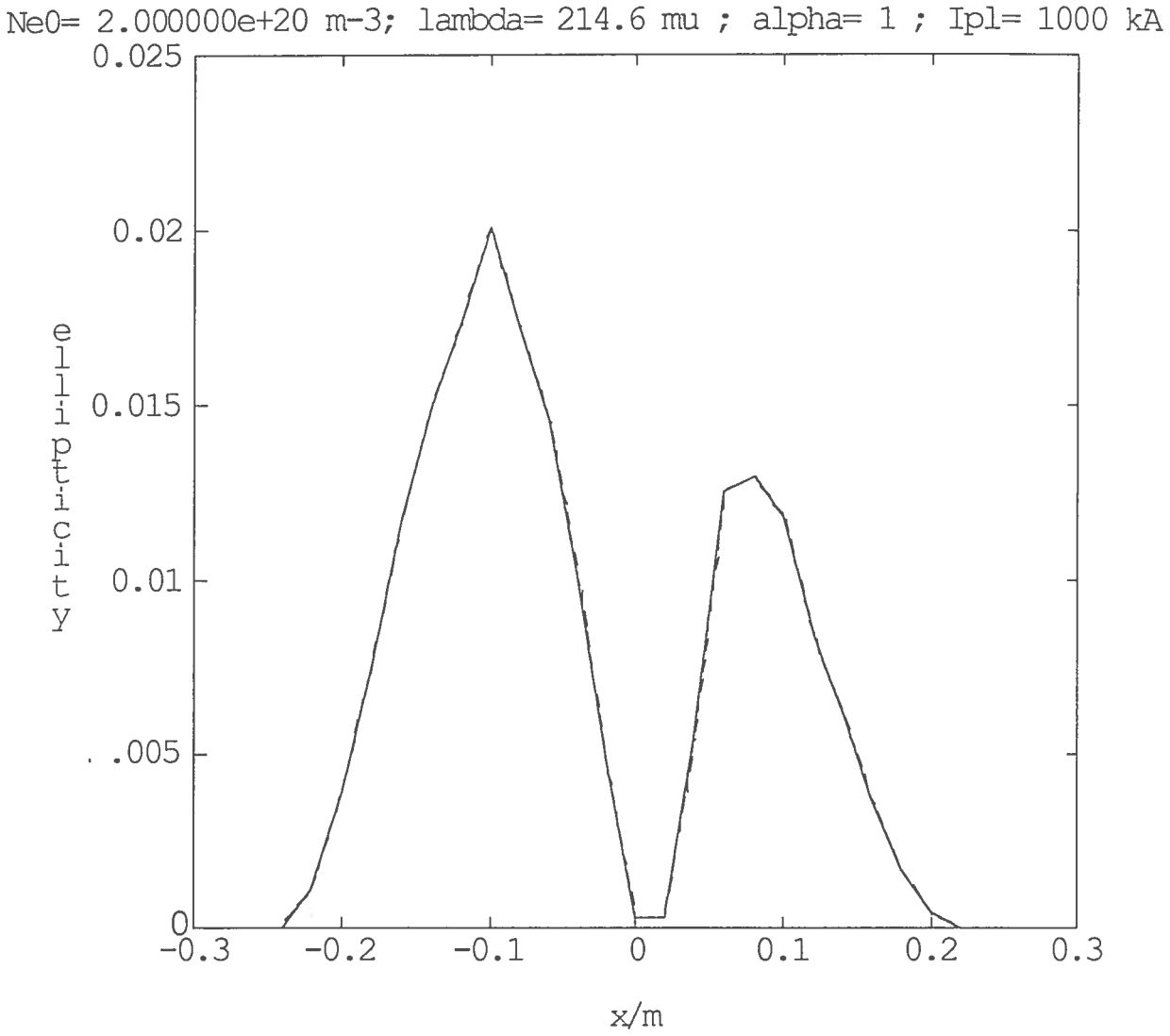

Fig. 4 : Ellipticity induced by the toroidal magnetic field for a high density elliptical 1MA TCV plasma (see fig.1), l=214.6μm. Beam enters the plasma as ordinary or extraordinary beam.

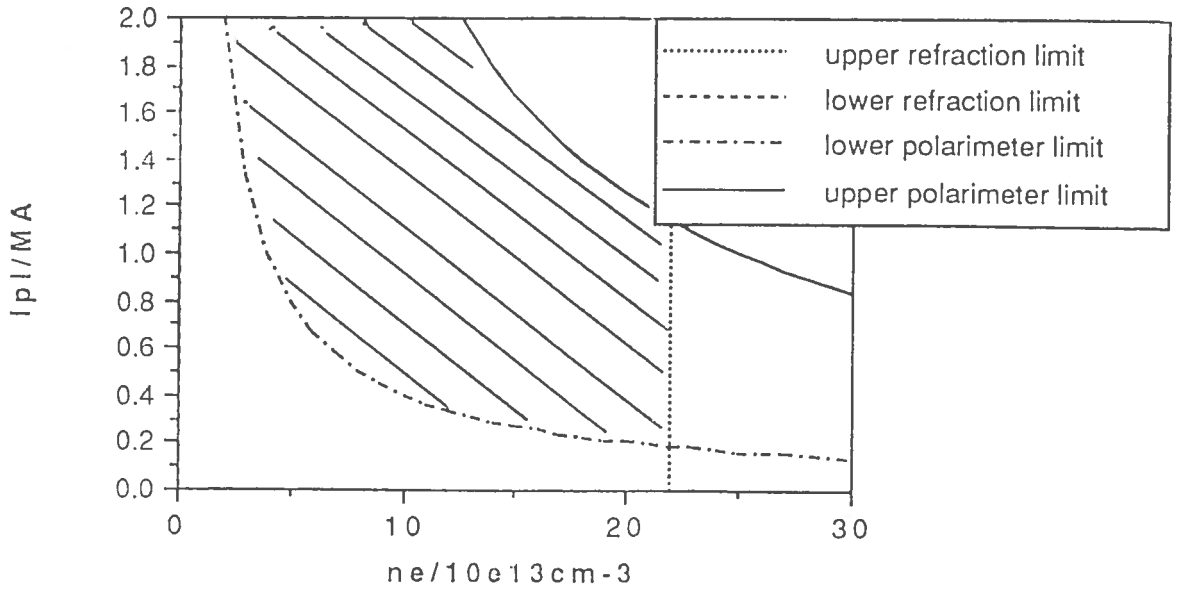

Fig. 5: Operational regime for an interferometer/polarimeter operating at 214.6μm (upper refr. limit : 20mm refraction, lower refr. limit : vibration limit, lower pol. limit : 6° rot. angle, upper pol. limit : 45° rot.angle (larger than in the text))

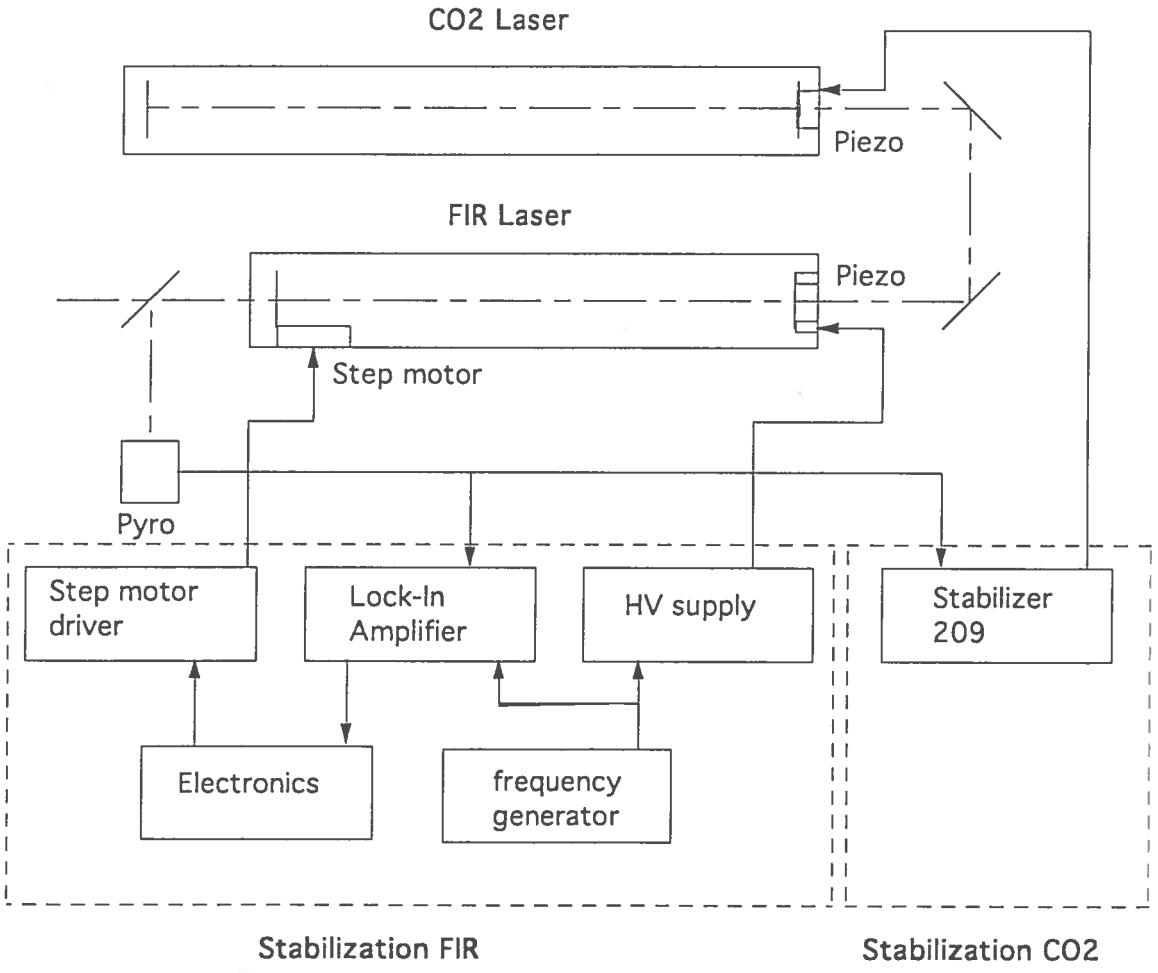

Fig. 6 : The laser system for the TCV interferometer

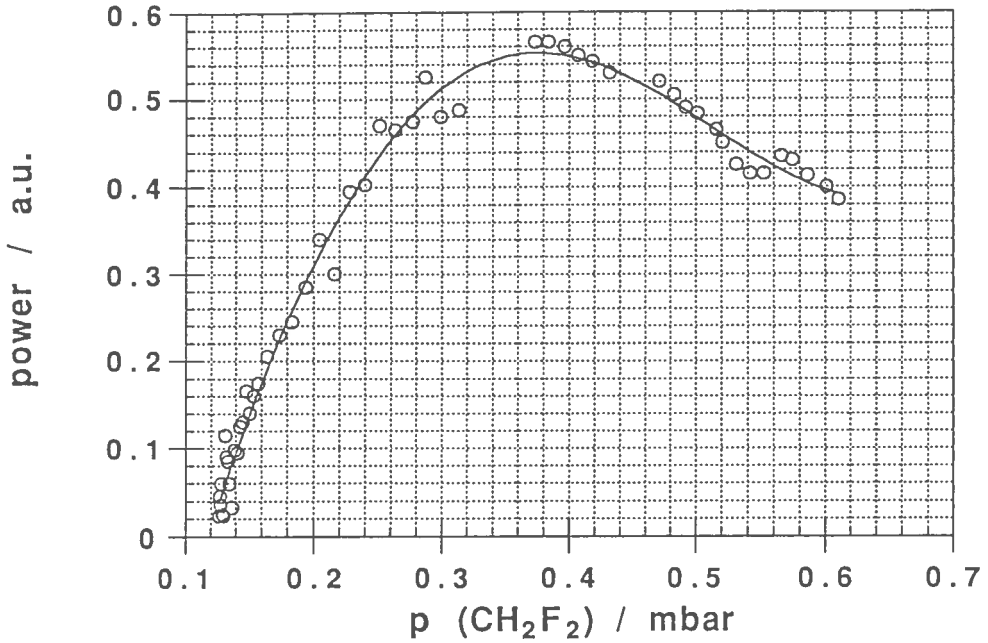

Fig. 7 : FIR power at 214.6μm as a function of the CH_2F_2 pressure in the FIR laser

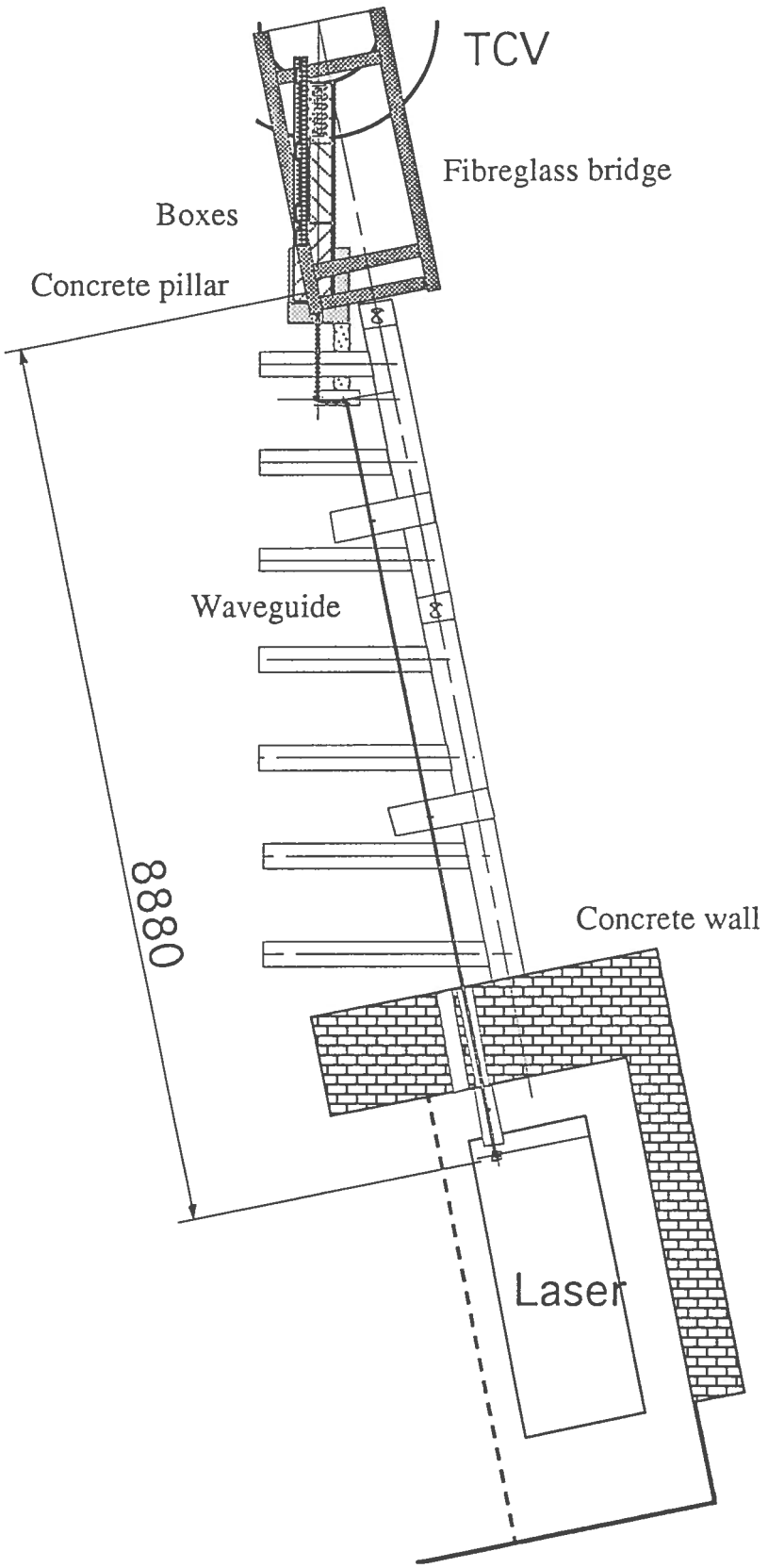

Fig. 8 : Setup of the laser system, the support structur at TCV and the boxes containing the optics, view from the top.

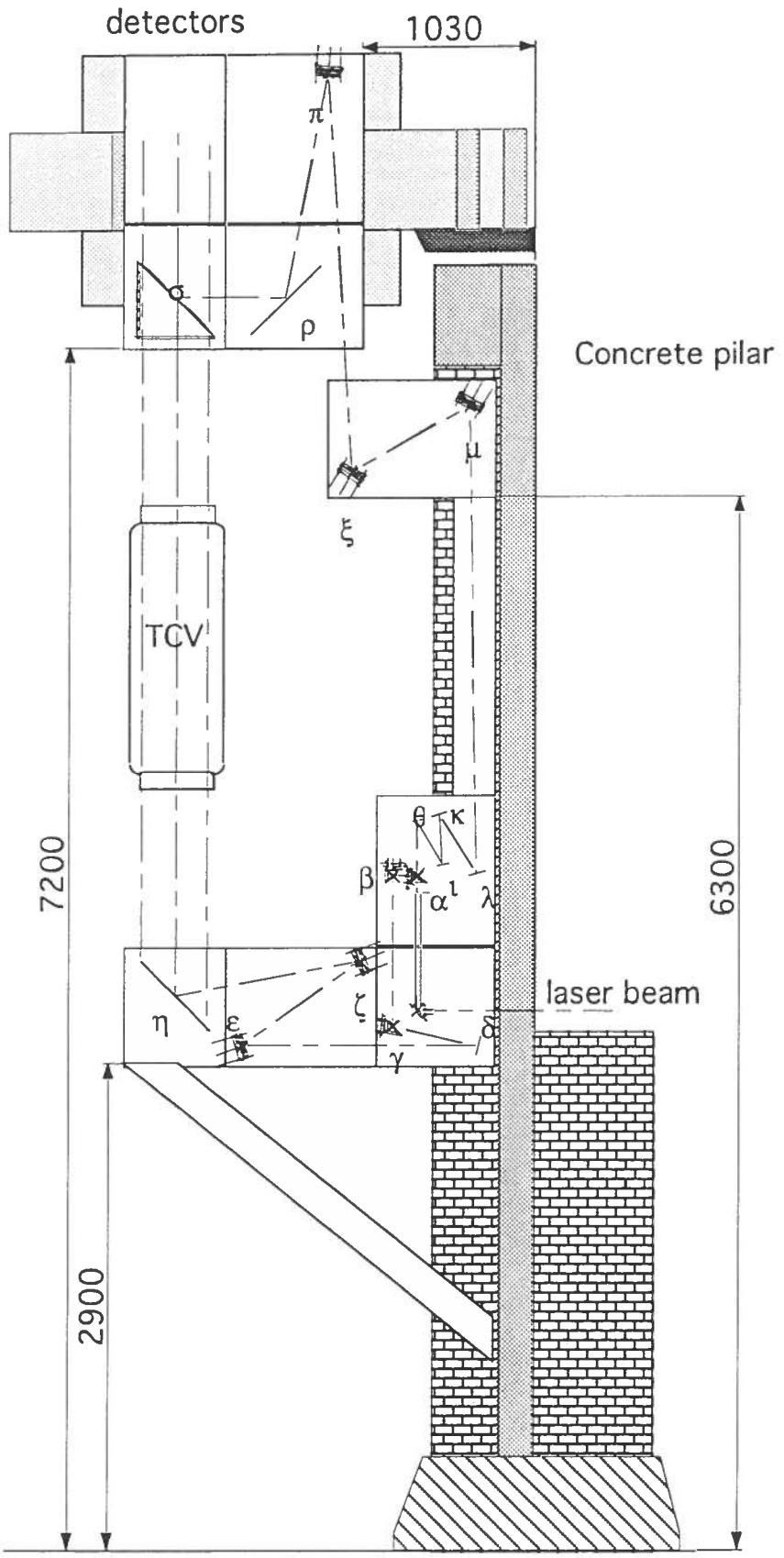

Fig. 9 : The support structur at TCV and the boxes containing the optics, view from the side.

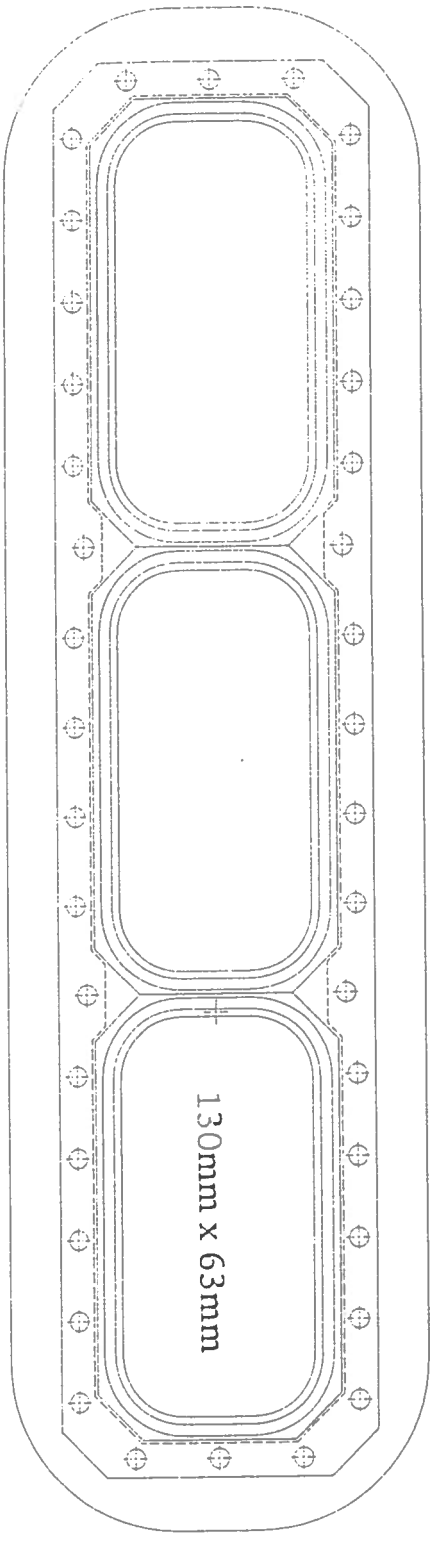

Fig. 10 : Window at TCV for the interferometer beam.

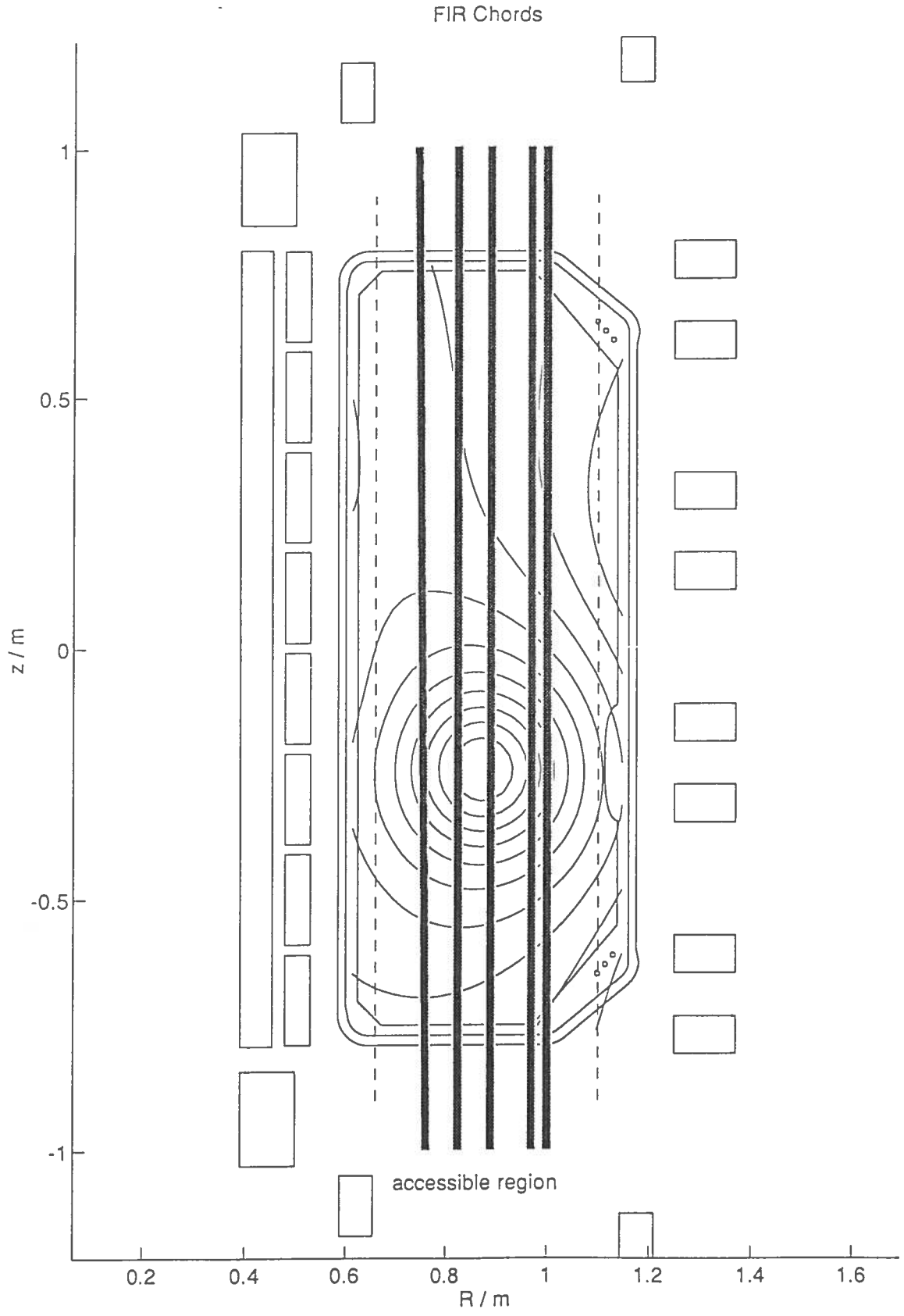

Fig. 11 : Cross-section of TCV in the interferometer sector.

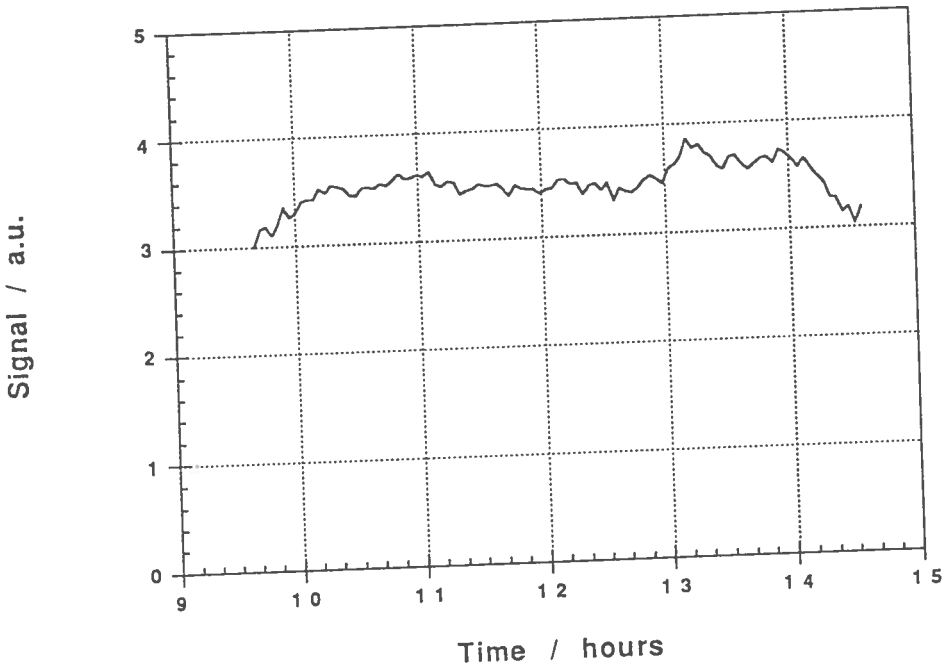

Fig. 12 : Amplitude of the beat signal on a central detector over an entire day

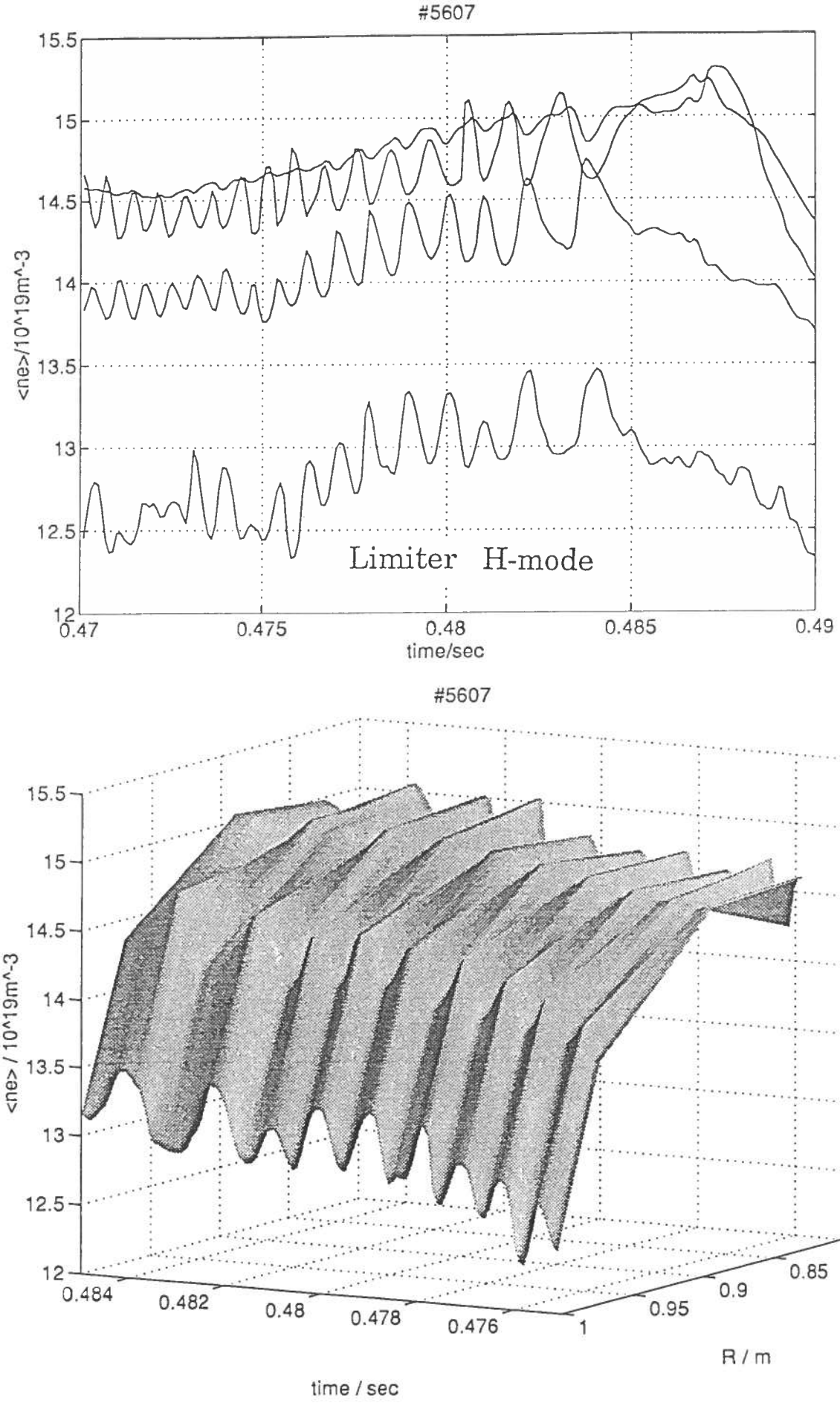

Fig. 13 :Locked mode in a limiter H-mode plasma. Traces 2,3,4 (central),5 from bottom to top on the right edge of the plot

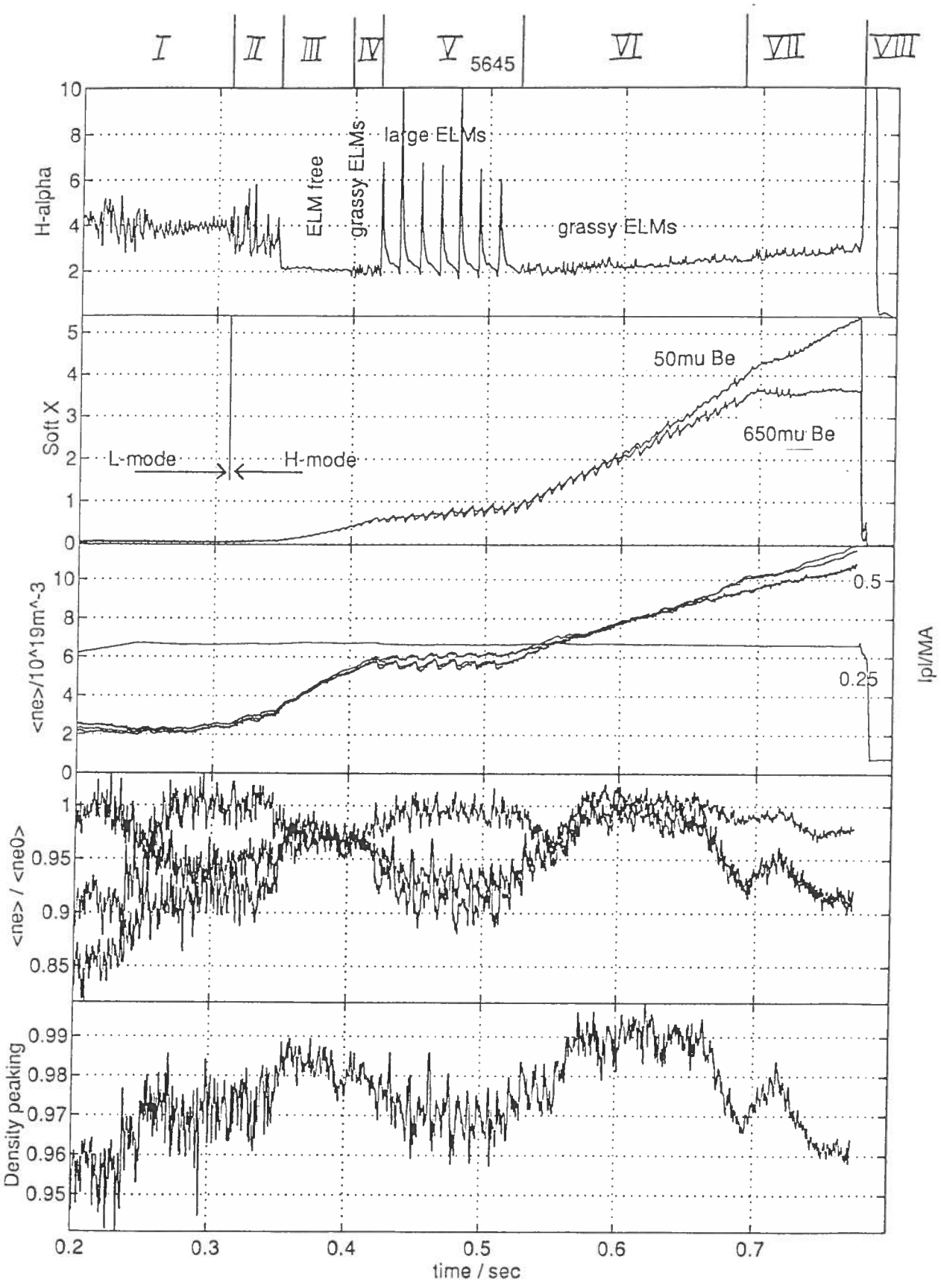

Fig. 14 : H-mode plasma. Flattening of the profile during beginning of the H-mode. Profile peaking by ELMs and in late H-mode.

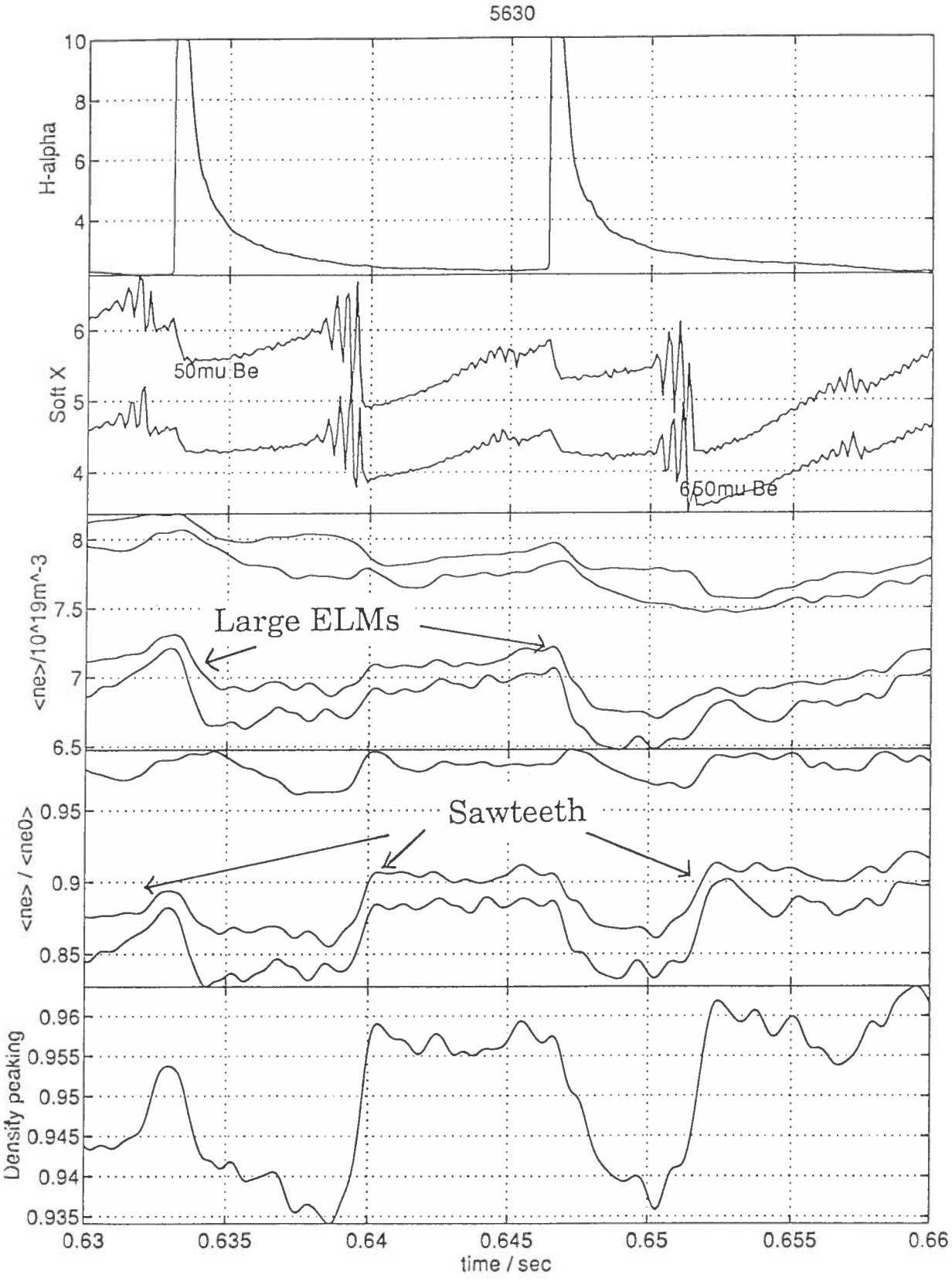

Fig. 15 : Profile behaviour during ELMs and sawteeth: ELMs peak and sawteeth flatten the profile.

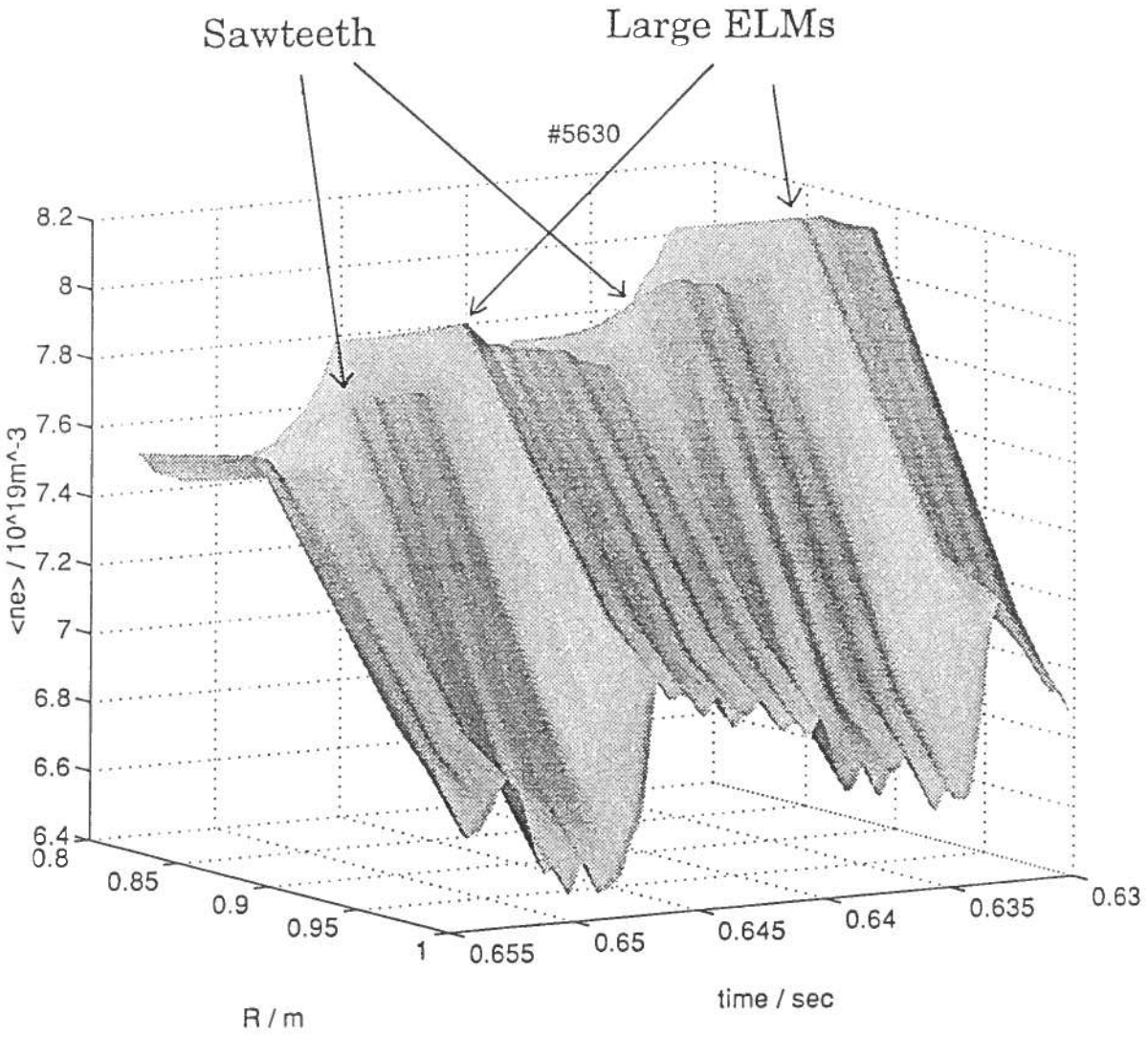

Fig. 16 : 3-D representation of figure 15.